

# Non-Markovianity during the quantum Zeno effect

A. Thilagam

*Information Technology, Engineering and Environment,  
Mawson Institute, University of South Australia, Australia 5095*

(Dated: April 26, 2022)

We examine the Zeno and anti-Zeno effects in the context of non-Markovian dynamics in entangled spin-boson systems in contact with noninteracting reservoirs. We identify enhanced non-Markovian signatures in specific two-qubit partitions of a Bell-like initial state, with results showing that the intra-qubit Zeno effect or anti-Zeno effect occurs in conjunction with inter-qubit non-Markovian dynamics for a range of system parameters. The time domain of effective Zeno or anti-Zeno dynamics is about the same order of magnitude as the non-Markovian time scale of the reservoir correlation dynamics, and changes in decay rate due to the Zeno mechanism appears coordinated with information flow between specific two-qubit partitions. We extend our analysis to examine the Zeno mechanism-non-Markovianity link using the tripartite states arising from a donor-acceptor-sink model of photosynthetic biosystems.

PACS numbers: 03.65.Yz, 03.65.Xp, 03.65.Ta, 03.67.Mn, 42.50.Lc, 71.35.-y

## I. INTRODUCTION

Quantum dynamical semigroups [1] operating via trace preserving, completely positive (CP) maps [2–4] with inbuilt divisibility [5–7], are well known to provide tractability when characterizing the evolution dynamics of memoryless quantum systems. These semigroups constitute the non commutative counterpart of classical Markov theories [8], and are based on contractions of density operators embedded either in the Hilbert space of Hilbert-Schmidt operators [1] or the Banach space of trace-class operators [9, 10], and involve the forward composition law. Recently, studies of the non-Markovian dynamics of evolution in open quantum systems [6, 7, 11, 12] have attracted increased attention as the Markovian model breaks down in the strong system-environment coupling regime or when un-factorized initial conditions exist between the system and environment [13–17], and for which a statistical interpretation of the density matrix is not guaranteed. In these instances, there is violation of complete positivity of the reduced dynamics of the quantum system depending on mathematical mappings known as the assignment or extension maps [14, 18, 19]. These maps provide description as to how a subsystem is embedded within a larger system, and can assume negative values for some correlated states. The quantum system may then evolve with signatures of non-Markovian dynamics with novel features of decoherence and non-invariant states even when an equilibrium point is reached. The non-invariant states here refer to states which occupy a subspace that is in a state of transience, arising from the presence of dissipative elements.

Due to the varying characteristics of different distance measures (e.g. trace distance, Bures distance, Hilbert-Schmidt distance [4, 20]), there is no single quantifiable measure, or a unique definition of non-Markovianity in quantum systems. In general, measures of non-Markovianity are based on deviations from the continuous, memoryless, completely positive semi-group feature of Markovian evolution. Both the concepts of divisibility [5, 7] and distinguishability [6] have been used to define non-Markovianity, and in particular the trace distance [6],  $D[\rho_1, \rho_2]$  is a well accepted metric measure of distinguishability of two quantum states  $\rho_1, \rho_2$ , that can be used to check the violation of the complete positivity during the time-evolution of a quantum system. During the time-evolution of a quantum state under the trace-preserving CP map  $\rho(0) \mapsto \rho(t) = \Phi(t, 0)\rho(0)$ , the trace-distance does not increase with time and  $D[\rho_1(t), \rho_2(t)] < D[\rho_1(0), \rho_2(0)]$ . Such a monotonically contractive feature is typical of a divisible Markovian mapping on the operator space, and the distinguishability between any states is bounded by its value at the initial state. An increase of trace distance during a time intervals is thus taken as a signature (sufficient but not necessary) of the attributes of non-Markovianity.

One area in which non-Markovian signatures has potential applications is in the quantum Zeno effect [21], which describes the retarded time evolution of a quantum state subjected to frequent measurements. In the limiting case of infinitely frequent observations, a scenario that is physically unattainable on the basis of the Heisenberg uncertainty [22], further decay is inhibited and the time evolution of the state comes to a standstill. The opposite effect which leads to enhancement in time evolution is known as anti-Zeno effect [23]. The theoretical formulations of the Zeno effect, which arises naturally from the quadratic short-time behavior of quantum evolution have been advanced considerably by Misra and Sudarshan [24] and Facchi and Pascazio [25–27]. The concept that a measurement process can decompose the total Hilbert space into partitions of orthogonal quantum Zeno subspaces has been examined via the adiabatic theorem [25, 26], as an extension of the Misra and Sudarshan theorem [24]. Under this scheme, the initial state is confined to single-dimensional invariant subspace, and its survival probability remains unchanged over

a period of time. Accordingly, different outcomes are eliminated and the system evolves within the same subspaces confined by the total Hilbert space. However it is also possible as in Schwinger's non-selective measurements [28], where projections onto multidimensional subspaces are involved, that a quantum system may be steered away from its initial state [29].

In this paper, we examine the Zeno dynamics of quantum systems from a quantum information perspective, by analyzing the behavior of dynamical semigroups during occurrence of Zeno and anti-Zeno effects. There are motivations to pursue this line of investigation due to the central role played by the decay process during Zeno/anti-Zeno effect. It is known that in unstable systems, the occurrence of both effects depend on critical parameters such as measurement frequencies and environmental noise [30]. Several quantum systems exhibit a combination of Zeno and anti-Zeno effects [31] such as the nanomechanical oscillator [32], disordered spin systems [33] and localized atomic systems [34]. The reversal in decay, which is apparent when the system shifts from displaying the anti-Zeno effect to the Zeno effect, necessitates some degree of reversibility during quantum evolutions. It is currently not clear as to the precise nature of the entities involved during these exchanges, however such reversals may be linked to feedback mechanisms within the open quantum system-reservoir model. This has implications for the semigroup law and contractions in the Hilbert space of Hilbert-Schmidt operators [1], with likely violations of forward time translations.

While the evolution within the projected (Zeno) subspace may be unitary, the overall dynamics appears complex due to non-Markovian dynamics. The latter feature may be exploited to explore potential applications in quantum control [35, 36] and information processing [37] involving periodic measurements, which can produce either a Zeno effect or an anti-Zeno effect, depending on the parameters of the system. The possibility of protecting quantum states via the Zeno effect has been shown in earlier works [38–40]. In this work, we highlight the appearance of non-Markovian signatures during the Zeno and anti-Zeno dynamics in specific two-qubit partitions of the spin-boson-reservoir system, with a broader aim of demonstrating that the context of non-Markovianity can reveal an alternative phenomenological perspective of the quantum Zeno effect.

Due to advancement in femtosecond based spectroscopy, there is currently great interest in the quantum processes which underpins quantum coherences and the exceptionally high efficiencies of energy transfer observed in light-harvesting systems [41–45]. Accordingly, we examine the occurrence of an environment induced quantum Zeno effect associated with dissipative photosynthetic sinks. The sinks form an integral component of the reaction centers (RC) in light-harvesting systems [41] by acting as regions where chemical energy is generated. In this study, we redefine the role of photosynthetic sinks as detectors of the excitation that is propagating through the system, and examine the impact of the Zeno effect on energy transfer mechanisms. Such effects are not thoroughly explored in biochemical systems, and the physical insight obtained from such studies is expected to provide useful information related to the quantum control of energy propagation process in artificial light-harvesting systems.

This paper is organized as follows. In Section II, we present several basic elements involved in the dynamics of open quantum systems on qualitative terms, with emphasis on the role of assignment maps in determining the nature (completely positive, positive and negative) of dynamical maps. A brief description of the pathological elements in density matrix operators due to initial system-reservoir interactions is also provided in Section II. In Section III we present a review of Sudarshan and Misra [24] formulations of the Zeno dynamics of quantum systems. In Section IV, we introduce a criteria to detect non-Markovianity in Zeno dynamics, and which will be used to analyze information flow in the spin-boson-reservoir system (described in Section V). Numerical details of the inter-qubit non-Markovianity during intra-qubit Zeno/anti-Zeno effect are provided in Section VI. Using a redefined non-Markovianity measure for a tripartite state, the Zeno mechanism in the photosynthetic reaction center (RC) is examined in Section VII. We present our main results and conclusions in Section VIII.

## II. DYNAMICS OF OPEN QUANTUM SYSTEMS AND ASSIGNMENT MAPS

In the standard approach involving open quantum systems to model dissipative and decoherence processes with memoryless time evolution, it is convenient to represent quantum states via normalized density matrices,  $\rho$ , which are hermitian ( $\rho = \rho^\dagger$ ), and positive definite. The positive definite attribute ensures that density matrices possess eigenvalues that are non-negative ( $0 \leq \lambda_i \leq 1$ ) and sum to unity ( $\text{Tr}(\rho)=1$ ) in the complex vector space of the Hilbert space,  $\mathcal{H}$ . Density operators have the advantage of being able to provide information on the fraction of ensemble systems which exist in a given state, when a large number of systems are under study. If  $\rho$  is representative of a pure ensemble, then  $\rho^2 = \rho$ , and in the case of a mixed ensemble, we obtain  $0 < \text{Tr}(\rho^2) < 1$ . To be identifiable in experimental setups, density matrices have to satisfy the complete positivity condition in which positive states are mapped into positive states. For states which can be expressed in a factorized density matrix form of a tensor product state with environment at initial time  $t=0$ , a dynamical evolution to the final state occurs in a tractable form. Here the link between initial and final state of the system can be specified by a semigroup of completely positive dynamical maps that ensure that the state operators retain a probabilistic interpretation. The possibility of occurrence of a

collection of (not uniquely) Kraus operators [3], is only guaranteed by completely positive maps so that the associated physical process can still continue to be described by CP maps

$$\rho' = \Lambda(\rho) = \sum_a K_a \rho K_a^\dagger. \quad (1)$$

where the Kraus operators  $K_a$  satisfy the completeness relation,  $\sum_a K_a^\dagger K_a = \mathbb{1}$ , and the map is trace preserving. Using the properties of a semigroup of completely positive dynamical maps, a quantum Markovian master equation of the Lindblad form, and which describes the time evolution of the reduced open system states has been obtained as [10, 46] :

$$\frac{d}{dt}\rho(t) = -i[\mathcal{H}, \rho(t)] + \sum_{k,l=1}^d \mathcal{L}_{kl}(\rho(t)) \quad (2)$$

$$= -i[\mathcal{H}, \rho(t)] + \frac{1}{2} \sum_{k,l=1}^d a_{kl} \left( 2\chi_k \rho(t) \chi_l^\dagger - \{\chi_k^\dagger \chi_l, \rho(t)\} \right), \quad (3)$$

$$= -i[\mathcal{H}, \rho(t)] + \sum_{k=1}^d \gamma_k \left( \mathcal{L}_k \rho(t) \mathcal{L}_k^\dagger - \frac{1}{2} \{\mathcal{L}_k^\dagger \mathcal{L}_k, \rho(t)\} \right), \quad (4)$$

where the Lindblad operators,  $\mathcal{L}_{kl}$  ( Eq. (2)) generate the map from the initial to the final density operators of  $\rho$ .  $\mathcal{H}$  arises from a combination of the isolated system Hamiltonian,  $\mathcal{H}_s$  and a system-environment interaction operator.  $\{\chi_k\}_{k=0}^d$  form the basis in the linear operator space, with  $\chi_0 = \mathcal{I}$  denoting the identity. The terms ( $a_{kl}$ ) in Eq. (3) constitute the positive definite  $d$ -dimensional Hermitian Gorini-Kossakowski-Sudarshan matrix  $\mathcal{A}$  [46], with a spectrum characterized by the decay terms,  $\{\gamma_k\}$ . The first term in Eq. (3) (or (4)) represents reversibility in system dynamics, while the symmetrized Lindblad operators are denoted by  $\mathcal{L}_k$ , in which both an operator and its hermitian conjugate are labeled by  $k$ . The latter incorporate environmental effects within the Born-Markov approximation and therefore act as the source of non-unitary dynamics.

While the Lindblad form in Eq. (4) ensures the positivity of density operators at any time, it is stringent in being applicable only to weak system-reservoir coupling when Markov approximation holds, greatly simplifying the mathematical structure of the mapping procedure. Eq. (4) is therefore not representative of situations when complete positivity of density operators is not a necessary feature. There are positive maps where *not all* eigenvalues of the mapped density operators are positive, and positive states continue to be mapped into positive states. And there are non-positive maps in which the positive states are mapped into negative states with at least one negative eigenvalue. As pointed out in the Introduction, the latter may arise when the system and its environment are initially correlated. Pechukas [14] first raised the possibility that non-Markovianity may result as an artifact of the product of the initial conditions,  $\rho_s(0) \otimes \rho_r(0)$ , where  $\rho_s$  ( $\rho_r$ ) denote the density operator specific to the system,  $s$  (reservoir,  $r$ ). In this regard, the Agarwal-Redfield (AR) equation of motion is seen to violate simple positivity in the semigroup form of Lindblad for certain initial states [47, 48].

The Agarwal bath [47] was also noted to produce spurious effects in the form of density matrix negativity for a range of initial conditions at low temperatures [49]. Such violations may occur in the initial stage of evolution dynamics due to backflow of information from the reservoir bath at short times comparable to the bath memory time [50]. The Lindblad form fails in these situations and it may be appropriate to use a non-Lindblad set of relations to describe the system dynamics during the initial period of quantum evolution, in which the finite time-scale of the vibrational environment becomes relevant. In this regard, the non-perturbative hierarchical equations of motion (HEOM) technique [51, 52] which incorporates higher vibrational energies in the bath as well as a finite time scale of the dynamics in the vibrational environment may provide a suitable alternative, as it is dependent on a second-order cumulant expansion that is exact for a harmonic bath.

There has been much debate on the occurrence of the non-positivity attribute in dynamical maps [13, 14, 18, 19, 53], with justifications provided [19, 53] to show that maps need not necessarily be in a completely positive form to describe the evolution of open quantum systems. The physical interpretation [19, 53] of non-positive maps has been linked to mathematical mappings known as assignment maps [14]. However there still seem to be a view that any physical evolution of reduced density operator MUST preserve positivity, and a violation of the complete positivity is considered to be unphysical, for which quantum trajectories lack a physical interpretation. These views are consistent with Alicki's [18] stand that "the complete positivity of the reduced dynamics should be and can be preserved." However this reasoning has been refuted by Pechukas [19] on the basis of improper use of "assignment maps" outside the weak coupling regime in Ref.[18]. Non-positivity features are of relevance in experimental techniques involving quantum process tomography in systems that possess initial correlations with the environment. The dependence of

positivity of the map on the interplay between the assignment map and the system-environment coupling has been recently shown [54], with conditions for positivity noted to arise from correlated system-environment states. Using the concept of assignment maps, an earlier work [53] examined the physical consistency of states for which the dynamical map is not positive. Such states were seen to be not amenable to the partial trace operation of extended systems which include specific correlations. The term ‘‘compatibility domain’’ was introduced [53] to describe the set of states for which non-positivity is physically valid. In forthcoming sections, we use numerical results to show the occurrence of non-Markovian dynamics in two model systems which incorporate Zeno dynamics. The time domains involved during effective Zeno or anti-Zeno dynamics are reasonably matched with the non-Markovian time scale of the reservoir correlation dynamics. In the next Section we provide the basics of the Zeno effect.

### III. ZENO DYNAMICS AND NON-MARKOVIANITY

The Kraus operators in Eq.(1) may be taken as measurement operators, and generalized measurements may be represented by a set of linear maps, where the action of each individual map acting on the density matrix may not preserve its trace [55]. Here we adopt Sudarshan and Misra [24] formulations of the Zeno dynamics of quantum systems, in which measurement in the Hilbert space  $\mathcal{H}$  are implemented via a Von Neumann projection operator  $\mathcal{P}$  (which may be one- or higher dimensional) with the Hilbert space range,  $\mathcal{H}_{\mathcal{P}}$ . An initial density matrix  $\rho_0$  of system  $S$  in  $\mathcal{H}_{\mathcal{P}} = \mathcal{P}\mathcal{H}$  satisfies  $\rho_0 = \mathcal{P}\rho_0\mathcal{P}$ ,  $\text{Tr}[\rho_0\mathcal{P}] = 1$ . In the absence of any measurement, the state evolves as [24, 26]

$$\begin{aligned}\rho(t) &= U(t)\rho_0U^\dagger(t) \\ U(t) &= \exp(-i\mathcal{H}^*t)\end{aligned}\tag{5}$$

where  $\mathcal{H}^*$  is a time-independent Hamiltonian with a lower bound. The probability that the system remains within  $\mathcal{H}_{\mathcal{P}}$  is given by  $P(t) = \text{Tr}(U(t)\rho_0U^\dagger(t)\mathcal{P})$ . In the event of measurement at time  $\tau$ , the density matrix  $\rho(\tau)$  transforms as  $\rho(\tau) = \frac{1}{p(\tau)}\mathcal{P}U(\tau)\rho_0U^\dagger(\tau)\mathcal{P}$ , where the survival probability within the subspace of  $\mathcal{H}_{\mathcal{P}}$  appear as [24, 26]

$$p(\tau) = \text{Tr}(V(\tau)\rho_0V^\dagger(\tau))\tag{6}$$

and  $V(\tau) \equiv \mathcal{P}U(\tau)\mathcal{P}$ . In the case of measurements taken at time intervals  $\tau = t/N$ , the survival probability of the quantum state,  $\rho(t/N)$  after  $N$  measurements appear as (c.f Eq.(6)) as

$$p(t/N) = \text{Tr}\left(V(t/N)^N\rho_0[V(t/N)]^{N\dagger}\right)\tag{7}$$

At very large  $N$ , transitions outside  $\mathcal{H}_{\mathcal{P}}$  are prohibited, and  $p(\frac{t}{N}) \rightarrow 1$ , so that the monitored system persists in the original state giving rise to the Zeno effect. Misra and Sudarshan [24] showed the semigroup properties of the operator  $V(t) \equiv \mathcal{P}U(t)\mathcal{P}$  at  $N \rightarrow \infty$ , at real time,  $t$ .

The projection-operator partitioning method introduced by Feshbach [57], divides the total Hilbert space of  $\mathcal{H}$  into two orthogonal subspaces generated by  $\mathcal{P}$  and its complementary projection operator  $\mathcal{Q} = 1 - \mathcal{P}$ . We note, following Eq.(7), that there exists a probability  $q(t/N) = (1 - p(t/N))$  that the quantum system has made a transition outside  $\mathcal{H}_{\mathcal{P}}$  to its ortho-complement,  $\mathcal{H}_{\mathcal{Q}}$ . We consider that the subspace of  $\mathcal{H}_{\mathcal{P}}$  is spanned by  $(|1\rangle_p, |0\rangle_p)$ , while that of  $\mathcal{H}_{\mathcal{Q}}$  is spanned by  $(|1\rangle_q, |0\rangle_q)$ . Accordingly,  $|1\rangle_p$  denotes the ‘‘survived’’ state due to measurement, while  $|1\rangle_q$  is the ‘‘un-survived’’ state. The measurement related decoherence due to leakages between subspaces may be associated with quantum jump operators involved in the transfer of states from  $\mathcal{H}_{\mathcal{P}} \rightarrow \mathcal{H}_{\mathcal{Q}}$ . The action of these random jump operators form the basis of the quantum trajectory approach [58], where the density operator is derived from an ensemble average of a range of conditioned operators [58] at the select time  $t$ .

We consider an initial state which starts from  $\mathcal{H}_{\mathcal{P}}$  at  $t=0$ , which is applicable to the composite state,  $|\psi_t\rangle = |1\rangle_p \otimes |0\rangle_q$ . After  $N$  measurements during a time duration,  $t$ , the system evolves according to the quantum trajectory dynamics model [58]

$$|\psi_t\rangle = \sqrt{p(t/N)}|1\rangle_p|0\rangle_q + \sqrt{q(t/N)}|0\rangle_p|1\rangle_q,\tag{8}$$

where  $\sqrt{p(t/N)}$  ( $\sqrt{q(t/N)}$ ) is the probability amplitude associated with the state residing in the subspace generated by  $\mathcal{P}$  ( $\mathcal{Q}$ ). To simplify the analysis, we assume that the concurrent occupation of states in the two subspaces is not viable during the evolution in Eq.(8). While a trace preserving map is inherent in the unitary time-evolution between measurements in Eq. (8), non-Markovian dynamics may arise when leakages between different subspaces are taken into account. This possibility is an important consideration in this work, and in the analysis of the quantum Zeno effect in the context of non-Markovian evolution dynamics.

#### IV. CRITERIA TO DETECT NON-MARKOVIANITY IN ZENO/ANTI-ZENO DYNAMICS

Under a completely positive map, there occurs no improvement in the distinguishability of a set of states. Therefore a completely positive, trace preserving dynamical map of a Markovian evolution on the operator space,  $\rho(0) \mapsto \rho(t) = \Phi(t, 0)\rho(0)$ , is monotonically contractive with respect to the trace-distance,  $D[\rho_1, \rho_2] = \frac{1}{2}\|\rho_1 - \rho_2\|$ . Here  $\|A\| = \text{Tr}[\sqrt{A^\dagger A}]$  between two states  $\rho_1, \rho_2$ . The relation

$$D[\rho_1(t_f), \rho_2(t_f)] < D[\rho_1(t_i), \rho_2(t_i)], \text{ for } t_f > t_i \quad (9)$$

is useful in identifying violation of the monotonically contractive characteristic of divisible Markovian mapping on the operator space. We note that Eq.(9) may also imply, with the incorporation of an intermediate time  $t_m$ ,

$$D[\rho_1(t_f), \rho_2(t_f)] < D[\rho_1(t_i), \rho_2(t_m)], \text{ for } t_f > t_i, t_f > t_m \quad (10)$$

$t_m$  may not necessarily be the same as  $t_i$ , and Eq.(10) still applies to a completely positive, trace preserving dynamical map.

To establish a criteria for detecting inter-qubit non-Markovian dynamics, we consider two initial states which are subjected to measurements of varying time duration. The trace-distance between these two states is then monitored after increasing the measurement duration of both states by the same amount. To simplify the numerical analysis, and without loss in generality, we choose two initial states  $\rho_1(t_i) = \rho_1(0)$ ,  $\rho_2(t_i) = \rho_2(\tau_1)$ , one of which is subjected to measurements of the ideal time duration of  $\tau \rightarrow 0$ , and is therefore stagnant, while the other initial state is measured in intervals of  $\tau_1$  (which can be taken as variable). For the final states, we select  $\rho_1(t_f) = \rho_1(\tau_2)$ ,  $\rho_2(t_f) = \rho_2(\tau_1 + \tau_2)$ , which differ from their respective initial states by being subjected to measurements with interval duration that is increased by  $\tau_2$ . The specifics of this model is convenient for analysis as will be shown in Section V. In order to determine the occurrence of non-Markovian dynamics, we employ a difference function dependent on trace-distances

$$\Delta(\tau_1, \tau_2) = D[\rho_1(\tau_2), \rho_2(\tau_1 + \tau_2)] - D[\rho_1(0), \rho_2(\tau_1)], \quad (11)$$

Positive values of  $\Delta(\tau_1, \tau_2)$  marks the presence of non-Markovian processes due to underlying information flow from the environment back to the system, however we note the different context in which ‘‘non-Markovian’’ is used here (reliant on violation of the complete positivity attribute) as compared to a similar term adopted by the chemical physical community. In the latter case, the information flow from the environment back to the system, which is absent in the Born-Markov quantum master equation (QME), may appear within the Markovian quantum master equation by eliminating the Born approximation.

It is also important to note subtle differences between the terms, ‘‘violation of the complete positivity’’ and ‘‘non-Markovianity’’, as the occurrences of violations of a completely positive map serve only as a sufficient but not necessary signature of non-Markovianity. Moreover, non-violation of the positivity may not even indicate the presence of a Markovian evolution. This highlights the complex links between dynamical maps and non-Markovian dynamics. We next describe the spin-boson system which is used as a framework to demonstrate non-Markovian features of memory effects based on Eq.(11), and to seek differences between the Zeno and anti-Zeno quantum dynamics.

#### V. ZENO DYNAMICS IN THE SPIN-BOSON SYSTEM

The spin-boson Hamiltonian provides an exemplary dissipative model to examine interaction between a two-state subsystem and a thermal reservoir [59]. Here we consider the density matrix of a spin-boson system associated with the Liouville equation  $\frac{\partial \rho}{\partial t} = -i[\hat{H}_T, \rho(t)]$ , where the total Hamiltonian  $\hat{H}_T = \hat{H}_{\text{qb}} + \hat{H}_{\text{os}} + \hat{H}_{\text{qb-os}}$  and  $\hat{H}_{\text{qb}}$  of the two-level qubit assumes the form  $\hat{H}_{\text{qb}} = \hbar \left( \frac{\Delta\Omega}{2} \sigma_z + \Delta\sigma_x \right)$ . The Pauli matrices are expressed in terms of the two possible states ( $|0\rangle, |1\rangle$ ),  $\sigma_x = |0\rangle\langle 1| + |1\rangle\langle 0|$  and  $\sigma_z = |1\rangle\langle 1| - |0\rangle\langle 0|$ .  $\Delta\Omega$  is the biasing energy while  $\Delta$  is the tunneling amplitude.

Each spin qubit is coupled to independent reservoirs of harmonic oscillators,  $\hat{H}_{\text{os}} = \sum_{\mathbf{q}} \hbar\omega_{\mathbf{q}} b_{\mathbf{q}}^\dagger b_{\mathbf{q}}$ .  $b_{\mathbf{q}}^\dagger$  and  $b_{\mathbf{q}}$  are the respective creation and annihilation operators of the quantum oscillator with wave vector  $\mathbf{q}$ . The qubit-oscillator interaction Hamiltonian is linear in terms of oscillator creation and annihilation operators  $\hat{H}_{\text{qb-os}} = \sum_{\mathbf{q}} \lambda_{\mathbf{q}} (b_{\mathbf{q}}^\dagger + b_{\mathbf{q}}) \sigma_z$ . The term  $\lambda_{\mathbf{q}}$  denotes the coupling between the qubit and the environment and is characterized by the spectral density function,  $J(\omega)$ , which we assume to be of the low-frequency form

$$J(\omega) = \sum_{\mathbf{q}} \lambda_{\mathbf{q}}^2 \delta(\omega - \omega_{\mathbf{q}}) = \frac{2\Lambda\omega}{\omega^2 + \alpha^2}, \quad (12)$$

The coupling strength between the qubit and the environment,  $\Lambda$ , is a product of the reorganization energy and  $\alpha$ , the characteristic frequency of the bath.  $\alpha$  is related to the reservoir correlation time,  $\alpha = \frac{1}{t_b}$ , and we assume that  $\alpha$  is small compared to the qubit energy difference,  $\Delta\Omega$ . With the choice of energy unit,  $\Delta\Omega=1$ ,  $\frac{\Lambda}{\Delta\Omega^2}$  yields a measure of a coupling strength that is dimensionless.

We consider an initial state of the qubit with its corresponding reservoir in the vacuum state at equilibrium,  $|\phi_i\rangle = |1\rangle_s \otimes \prod_{k=1}^{N'} |0_k\rangle_r = |1\rangle_s \otimes |\mathbf{0}\rangle_r$  where  $|1\rangle_s$  ( $|0\rangle_s$ ) is the upper (lower) level of the qubit, and  $|\mathbf{0}\rangle_r$  implies that all  $N'$  wavevector modes of the reservoir are unoccupied in the initial state. During a measurement, a transition of a qubit from its excited state to ground state is triggered, which we consider to follow the simple mode of evolution as in Eq.(8),  $|\phi_i\rangle$  proceeds in time as

$$|\phi_i\rangle \longrightarrow u(t) |1\rangle_s |\mathbf{0}\rangle_r + v(t) |0\rangle_s |\mathbf{1}\rangle_r, \quad (13)$$

Thus we consider an evolution in which the excitation is present in one of the two subspaces as in Eq.(8). In order to keep the problem tractable we consider that  $|\mathbf{1}\rangle_r$  denotes a collective state of the reservoir,  $|\mathbf{1}\rangle_r = \frac{1}{v(t)} \sum_n \lambda_{\{n\}}(t) |\{n\}\rangle$  where  $\{n\}$  denotes an occupation scheme in which there are  $n_i$  oscillators with wavevector  $k = i$  in the reservoir and we define the state  $|\{n\}\rangle$  as  $|\{n\}\rangle = |n_0, n_1, n_2 \dots n_i \dots n_{N'}\rangle$ . In the case of ideal measurements, the functions  $u(t)$  and  $v(t)$  in Eq.(13) must always satisfy the relation  $u(t)^2 + v(t)^2 = 1$ , however this relation may be violated in the case of measurements which introduce significant level of disturbance to the system being monitored [60].

The survival probability associated with  $N$  measurements (see Eq.(13) for a single measurement) performed at regular intervals  $\tau$ ,  $P^N(t) = u(\tau)^{2N} = \exp(-\gamma(\tau)t)$  where  $t = N\tau$ . The effective decay rate,  $\gamma(\tau)$  at small values of  $\tau$  is obtained using ( $\Delta=2$ ,  $\hbar=1$ ) Kofman and Kurizky's formalism [23]

$$\gamma(\tau) = \int_0^\infty d\omega J(\omega) F_\tau(\omega - \Delta\Omega), \quad (14)$$

Facchi et. al. [61] made comparison of the effective decay rate  $\gamma(\tau)$  to the natural decay rate (without measurement), and attributed a smaller  $\gamma(\tau)$  than the natural decay rate to the Zeno effect while a larger  $\gamma(\tau)$  (than the natural decay rate) is linked with the anti-Zeno effect. The transition point occurs at the intersection of the effective decay rate and the natural one at a specific time known as jump time. Eq.(14) is dependent on the convolution of two main functions: (a) the modulating function  $F_\tau(\omega - \Delta\Omega)$  and (b) spectral density  $J(\omega)$ . The modulating function is given by

$$F_\tau(\omega - \Delta\Omega) = \frac{\tau}{2\pi} \text{sinc}^2 \left[ \frac{(\omega - \Delta\Omega)\tau}{2} \right] \quad (15)$$

and is associated with measurements at intervals of  $\tau$ . In the limit  $\tau \rightarrow 0$ ,  $F_\tau(\omega - \Delta\Omega) \rightarrow 0$ ,  $\gamma(\tau) \rightarrow 0$  which explains the emergence of the quantum Zeno effect that is independent of the spectral density  $J(\omega)$ .

A third term,  $f(\omega)$  that incorporates rotating and counter-rotating terms [62] introduces an overall shift in the effective decay rate, without greatly affecting further analysis of non-Markovianity with respect to the system parameters. We thus employ  $f(\omega)=1$  (the rotating wave approximation, RWA) to simplify the numerical analysis. We obtain the decay rate at the limit,  $\tau \rightarrow \infty$ , as  $\gamma_0 = \gamma(\tau \rightarrow \infty) \approx J(\Delta\Omega)$ . The quantum Zeno (anti-Zeno) effect occurs when  $\gamma(\tau) < \gamma_0$  ( $\gamma(\tau) > \gamma_0$ ). The parameter range of  $\tau$  and the  $\alpha$ , the characteristic frequency of the bath, for which these two distinct effects occur is shown in Figure 1. The quantum Zeno effect always occurs at very short  $\tau < 1$ , however beyond  $\tau > 1$  the characteristic frequency of the bath appears to influence the occurrence of the anti-Zeno effect at  $\alpha < 0.25$ .

While the decay rate itself is dependent on the coupling strength term  $\Lambda$ , the occurrence of Zeno or anti-Zeno effect is independent of  $\Lambda$ , this is partly due to the use of the rotating wave approximation. The influence of  $\Lambda$  in determining Zeno or anti-Zeno dynamics may resurface with removal of the latter approximation, however it is expected to be weak compared to the influence of  $\alpha$ , the characteristic frequency of the bath. This may be attributed to the non-Markovian times-scales at which Zeno dynamics operate. The results here (to be shown in Section VI) appear to be influenced strongly by  $\alpha$ , which controls the range of time scales to which the bath can respond, and which is intricately linked to measurements taken at intervals of  $\tau$ . The results in Figure 1 therefore highlight the critical role of  $\alpha$  in systems where the RWA can be justified. Moreover these findings suggest the relevance of the Zeno/anti-Zeno effect to inter-qubit non-Markovian dynamics rather than intra-qubit non-Markovianity, in structures with large network size and connectivity as is the case with the light-harvesting biochemical systems. We therefore examine the link between the inter-qubit Non-markovianity and the intra-qubit Zeno effect in a qubit pair system, next.

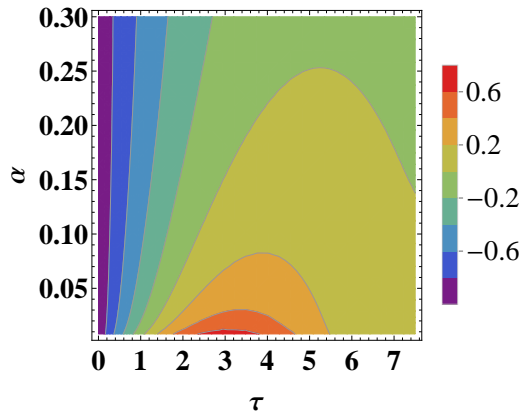


FIG. 1: Occurrence of the quantum Zeno effect or the anti-Zeno effect, based on the ratio of decay rates  $\frac{\gamma(\tau)}{\gamma_0}$ , as a function of measurement time duration  $\tau$  and  $\alpha$ , the characteristic frequency of the bath. The spectral density function,  $J(\omega)$  in Eq.(12) is numerically evaluated using a unit system in which  $\hbar=1$ ,  $\Delta = 2$  and  $\Delta\Omega=1$ . The quantum Zeno effect is marked by regions with negative values while the anti-Zeno effect is denoted by positive values. The occurrence of these effects are independent of the coupling strength,  $\Lambda$  (using RWA).

## VI. INTER-QUBIT NON-MARKOVINITY AND THE INTRA-QUBIT ZENO EFFECT IN A QUBIT PAIR SYSTEM

We now extend the composite system in Eq.(8) to examine the joint evolution of a pair of two-level qubit systems in uncorrelated reservoirs via the following Bell-like initial state

$$|\Phi\rangle_0 = [a|0\rangle_{q1}|0\rangle_{q2} + b|1\rangle_{q1}|1\rangle_{q2}]|0\rangle_{r1}|0\rangle_{r2}, \quad (16)$$

where  $i=1,2$  denote the two qubit-reservoir systems associated function  $u_i(t)$  in Eq.(13).  $a, b$  are real coefficients and satisfy,  $a^2 + b^2 = 1$ . Using Eq.(13) and tracing out the reservoir states we obtain a time-dependent qubit-qubit reduced density matrix in the basis ( $|00\rangle, |01\rangle, |10\rangle, |11\rangle$ ) which evolves with time duration  $\tau$  as

$$\rho_{q1,q2}(t) = \begin{pmatrix} f_1 & 0 & 0 & f_5 \\ 0 & f_2 & 0 & 0 \\ 0 & 0 & f_3 & 0 \\ f_5 & 0 & 0 & f_4 \end{pmatrix}. \quad (17)$$

where  $f_1 = a^2 + b^2v_1(\tau)^2v_2(\tau)^2$ ,  $f_5 = abu_1(\tau)u_2(\tau)$ ,  $f_2 = b^2v_1(\tau)^2u_2(\tau)^2$ ,  $f_3 = b^2u_1(\tau)^2v_2(\tau)^2$ ,  $f_4 = b^2u_1(\tau)^2u_2(\tau)^2$ . We assume that the usual unit trace and positivity conditions of the density operator  $\rho_{q1,q2}$  are satisfied. The reservoir-reservoir reduced density matrix  $\rho_{r1,r2}$  is similarly obtained by tracing out qubit states. Each non-zero matrix term of  $\rho_{r1,r2}$  is easily obtained from the corresponding term  $\rho_{q1,q2}(t)$  by swapping  $u_i \leftrightarrow v_i$ . Both matrices possess the well-known  $X$ -state structure which preserve its form during evolution. Using Eq.(13) and tracing out the one qubit and reservoir state, we also obtain the inter-system qubit-reservoir density matrix  $\rho_{q1,r2}(t)$  of the same form as in Eq.(17), but one in which  $f_1 = a^2 + b^2u_1(\tau)^2v_2(\tau)^2$ ,  $f_5 = abu_1(\tau)v_2(\tau)$ ,  $f_2 = b^2v_1(\tau)^2v_2(\tau)^2$ ,  $f_3 = b^2u_1(\tau)^2u_2(\tau)^2$ ,  $f_4 = b^2u_1(\tau)^2v_2(\tau)^2$ .

In Figure 2, we have plotted the trace-distance difference function  $\Delta(\tau_1, \tau_2)$  (see Eq.(11)) as a function of  $\tau_1$  and  $\tau_2$  (using the qubit-qubit density matrix) at increasing values of  $\alpha$ , the characteristic frequency of the bath. We recall that  $\tau_1$  is inversely proportional to the measurement frequency of one of the initial state, while  $\tau_2$  is the increase in measurement time duration of the final states. We note the enhancement of inter-qubit non-Markovianity with increase in  $\alpha$ , (i.e. increased Zeno effect) at constant coupling strength,  $\Lambda$ . These results in combination with the earlier results obtain in Figure 1, show that the intra-qubit Zeno effect occurs in conjunction with inter-qubit non-Markovian dynamics. A decrease in decay rate is linked with reservoir feedback for the qubit-qubit subsystem.

In the case of the inter-system qubit-reservoir density matrix  $\rho_{q1,r2}(t)$ , we note that the inter-qubit non-Markovian dynamics is erased at  $\tau_1 < 0.1$  and enhanced at higher  $\tau_1 > 2$  with increase in  $\alpha$  (see Figure 3). The results in Figure 3 indicate increasing feedback into the qubit-reservoir subsystem, consistent with the intra-qubit anti-Zeno effect that

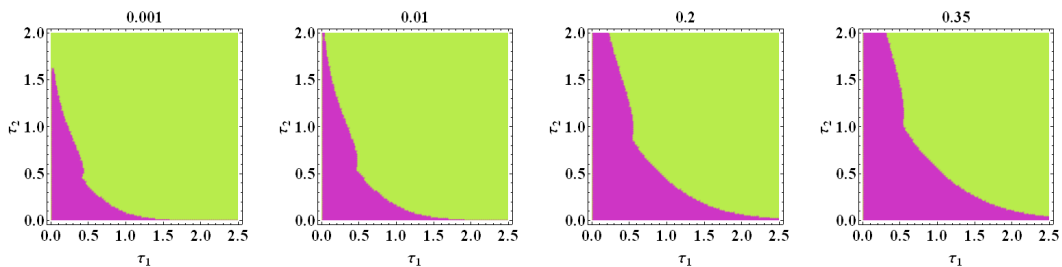


FIG. 2: Sign of Trace-distance difference function  $\text{Sign}[\Delta(\tau_1, \tau_2)]$  (see Eq.(11)) as a function of  $\tau_1$  and  $\tau_2$  evaluated for the reduced density matrix corresponding to the qubit-qubit subsystem (Eq.(17)).  $\text{Sign}[x]$  yields -1, 0, or 1 depending on whether  $x$  is negative, zero, or positive. Values of  $\alpha$ , the characteristic frequency of the bath is indicated at the top of each figure.  $a=b=\frac{1}{\sqrt{2}}$ , coupling strength  $\Lambda = 0.01$ , number of measurements  $N=20$ . Regions of non-Markovianity are shaded purple, while regions which are shaded green denote occurrence of Markovian evolution dynamics. Non-Markovianity increase occurs in conjunction with the Zeno effect for the qubit-qubit subsystem.

applies for the specified range of  $\alpha$  shown in Figure 1. The combined results of Figs 2 and 3 indicate that decrease (increase) in decay rate due to Zeno (anti-Zeno) effect may be linked to information flow between specific two-qubit partitions.

While the results obtained here are specific to the choice of the Bell-like initial state provided in Eq.(16), the output related to the degree of correlation or anti-correlation of the inter-qubit non-Markovianity with respect to the intra-qubit Zeno effect, will vary according to the choice of the initial state. The robustness of the connection between non-markovianity and Zeno effect is based on the area size of the non-Markovian region (i.e. the sign rather than the magnitude of the Trace-distance) which is evaluated numerically (coloured purple in Figures 2, 3). The determination of the size of this region as a function of the amplitude  $a$ , coupling function  $\alpha$ , and number of measurements  $N$  is expected to provide further information on the non-Markovian dynamics, but will be pursued elsewhere.

We tested the links between the Zeno/anti-Zeno effect and inter-qubit non-Markovianity for all possible two-qubit partitions possible within Eq.(16), and noted a definite dependence on the partition choice (qubit-qubit, reservoir-reservoir, qubit-reservoir) in relation to non-Markovian dynamics. We have focussed on the two main subsystems which showed significant contrasting modes of information flow with respect to changes in decay rate arising from Zeno or anti-Zeno effect. The results obtained here show that the bath memory time (as seen in changes due to  $\alpha$ ) plays a critical role in the non-Markovian processes of qubit-bath interaction, and may provide a basis for the Zeno effect-non-Markovianity link. There is approximate matching in the time domains involved during effective Zeno or anti-Zeno dynamics and the non-Markovian time scale of the reservoir correlation dynamics. We bear in mind that these results are obtained on the basis of the RWA and the assumption of a constant coupling strength,  $\Lambda$ . In the next Section, we consider a tripartite qubit state constructed from a simple model of the light-harvesting complex, accordingly we adopt slightly different criterias for determining the Zeno-effect and non-Markovian regions.

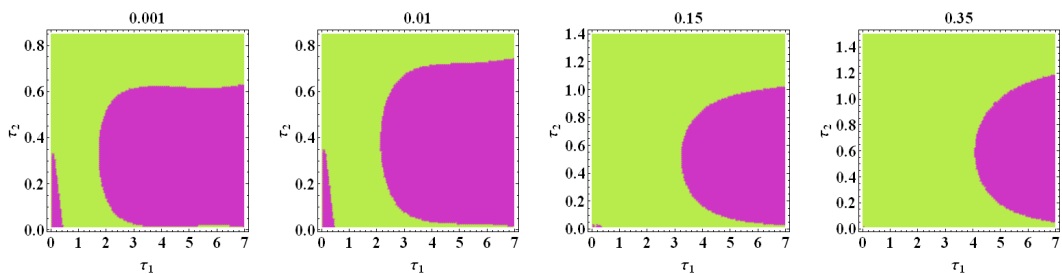


FIG. 3: Sign of Trace-distance difference function,  $\text{Sign}[\Delta(\tau_1, \tau_2)]$  as a function of  $\tau_1$  and  $\tau_2$  evaluated for the reduced density matrix corresponding to the inter-system qubit-reservoir density matrix  $\rho_{q_1, r_2}(t)$ . Values of  $\alpha$ , the characteristic frequency of the bath are indicated at the top of each figure.  $a=b=\frac{1}{\sqrt{2}}$ ,  $\Lambda = 0.01$ , number of measurements  $N=20$ . Regions of non-Markovianity are shaded purple, while regions which are shaded green denote occurrence of Markovian evolution dynamics. Areas of non-Markovianity increases with  $\alpha$  at higher  $\tau_1 > 2$ , while presence of non-Markovianity is erased for  $\tau_1 < 0.1$  for increasing  $\alpha$ .



## VII. ZENO EFFECT AT DISSIPATIVE SINKS IN THE PHOTOSYNTHETIC REACTION CENTER

It is well known [63–65] that several chemical and physics systems can be modeled using a reaction coordinate linked to an effective potential energy function with two distinct minima points, and which is amenable to analysis in terms of exchange of quantum correlations between the system under study and its immediate environment. The light harvesting complex is an important system where the observed long lived coherences, lasting several picoseconds, may be linked to quantum information processing features inherent in the propagating exciton (or correlated electron-hole pair). The biological pigment-protein complex, called FMO (Fenna-Matthews-Olson) trimer complex in the sulphur bacteria [41] constitutes three symmetrically equivalent monomer subunits. Each monomer unit is generally modeled as a network of eight bacteriochlorophyll (BChl)a molecules within a matrix of protein molecules. The series of excitonic exchanges between molecular sites is described by an exciton Hamiltonian of the form in Eq. (4). Local Lindblad terms which represent dephasing and dissipation processes linked to the surrounding environment are incorporated during the exchange mechanisms. The exciton energy is irreversibly transferred to a reaction center (RC), where it undergoes conversion into chemical energy.

Earlier works [44] examined the fine interplay between quantum coherence and environmental noise (both Markovian and non-Markovian) to achieve optimal functionality in photosynthetic systems. In a separate study [66], the non-Markovian processes were seen to be prominent in the reorganization energy regime, also noted by Silbey and coworkers [67] who showed that the reorganization energy and the bath relaxation rate played critical roles during the energy transfer process. Chen et. al. [68] presented results which showed the importance of incorporating the site energy based electronic coupling correlations. The increased oscillations of entanglement in the non-Markovian regime of intra-qubit systems in an earlier work [69] further highlighted the importance of feedback mechanisms in the FMO monomer system. However in all these works, there was focus only on the intra-qubit Markovian attribute, and to this end, the contributions from inter-qubit Markovian dynamics of photosynthetic systems need further study.

An important reason to consider inter-qubit Markovian dynamics is associated with the significance of multipartite states that act as sources of local and non-local correlations in large photosynthetic membranes which feature in many FMO complexes [69]. The intra-qubit Markovian (and non-Markovian) model, which is suitable for the FMO monomer, is less applicable in the examination of quantum correlations and exchanges across a wider networked molecular system with capacity to hold a large number of entangled excitonic qubits. The latter system may arise when entangled photons are absorbed by the photosynthetic membrane, setting up fruitful conditions for a system of initially correlated chromophores. In the FMO monomer, it was shown recently [43] that the unique location of the eighth chromophore (at site 8) gives rise to strong inter-monomer interactions, facilitating excitation transfer between monomers of the FMO trimer. Hence our approach focussed on inter-qubit non-Markovian dynamics is best suited to the realistic condition of an entire photosynthetic membrane constituting many FMO complexes and thousands of bacteriochlorophylls. In Section VI, we noted the time domains involved during effective Zeno mechanism appears matched with the non-Markovian time scale of the reservoir correlation dynamics. This points to the relevance of the inter-qubit Markovian dynamics in the context of the Zeno mechanism in applications related to light harvesting systems.

Here we utilize the tripartite states arising from a donor-acceptor-sink model to examine the subtle link between the intra-qubit Zeno effect and the inter-qubit non-Markovian dynamics. The Zeno criteria used is dependent on the indirect action of the dissipative sink on the non-Markovian dynamics of a specific inter-qubit system. The non-Markovianity is evaluated using the trace-distance difference measure of a tripartite state, these criterias therefore differ from those used in Section V. A prototypical energy transfer mechanism in light-harvesting systems is thus modeled via a photosynthetic reaction center (RC) consisting of the donor and acceptor protein pigment complexes and a third site acting as the phonon-dissipative sink with a continuous frequency spectrum. The energy from the acceptor is considered to dissipate into the phonon reservoir over time. The effective Hamiltonian,  $\hat{H}_T$ , which describes of the donor and acceptor coupled to the sink consists of an exciton at the donor site  $d$ , coupled to second exciton at the acceptor  $a$  site, which in turn is interacting with its own source of bosonic reservoir  $r$  ( $\hbar=1$ )

$$\hat{H}_T = \hat{H}_s + \hat{H}_r + \hat{H}_I \quad (18)$$

$$\hat{H}_s = \omega_d \sigma_+^d \sigma_-^d + \omega_a \sigma_+^a \sigma_-^a + V(\sigma_-^d \sigma_+^a + \sigma_+^d \sigma_-^a) \quad (19)$$

$$\hat{H}_r = \sum_k \omega_k b_k^\dagger b_k, \quad \hat{H}_I = \sum_{k=1}^N (\varphi_k \sigma_-^a \hat{b}_k^\dagger + \varphi_k^* \hat{b}_k \sigma_+^a), \quad (20)$$

where  $\omega_d$  ( $\omega_a$ ) is the exciton resonance frequency at the donor (acceptor) site,  $\sigma_+^d$  ( $\sigma_-^d$ ) denotes the raising (lowering) operator of the exciton [70] at the donor site, and  $\sigma_+^a$  ( $\sigma_-^a$ ) denotes the raising (lowering) operator of an exciton at the acceptor site. The operator  $\hat{b}_k$  ( $\hat{b}_k^\dagger$ ) annihilates (creates) a phonon with frequency  $\omega_k$  in  $k$ -th mode of the reservoir.  $V$

is the coupling constant between the acceptor and donor excitons and  $\varphi_k$  is the linear coupling between the exciton at the acceptor site and the phonon with frequency  $\omega_k$  in  $k$ -th mode.

Using Feshbach's projection-operator method [57], the total Hilbert space of  $\hat{H}_T$  is divided into two orthogonal subspaces generated by the projection operators,  $\mathcal{P}$  and  $\mathcal{Q}$  where  $\mathcal{Q} = 1 - \mathcal{P}$ . For the photosynthetic reaction center (RC),  $\mathcal{P} = \sigma_+^d \sigma_-^d + \sigma_+^a \sigma_-^a$  and  $\mathcal{Q} = \sum_k b_k^\dagger b_k$ , such that  $\mathcal{P}\mathcal{Q} = \mathcal{Q}\mathcal{P} = 0$ . The density operator associated with the qubit-cavity system is given by  $\rho_s(t) = \mathcal{P} \rho \mathcal{P}$ ,  $\rho$  being the density operator of the total system. Using a phenomenological master equation that incorporates only energy dissipation from the exciton at the acceptor site (with decay rate  $\lambda_c$ ), and providing for the presence of a reservoir system with a flat spectrum, the reduced density matrix,  $\rho_s$  is obtained as

$$\frac{d}{dt} \rho_s = i(\rho_s H'_s - H'_s \rho_s) + \lambda_c \sigma_-^a \rho_s \sigma_+^a, \quad (21)$$

$$H'_s = \omega_d \sigma_+^d \sigma_-^d + (\omega_a + \delta - i \frac{\lambda_c}{2}) \sigma_+^a \sigma_-^a + V(\sigma_-^d \sigma_+^a + \sigma_+^d \sigma_-^a) \quad (22)$$

where  $\delta$  arises due to energy renormalization, and the decay rate  $\lambda_c$  is influenced by the environmental bath parameters such as temperature and distribution profile of vibrational frequencies. Eq. (21) is equivalent to the Haken-Strobl model at infinite temperature, where pure dephasing is accounted for in terms of a classical, fluctuating field in the presence of a sink [67]. By setting the resonant condition  $\omega_d = \omega_a + \delta$ , and assuming the presence of the initial excitation to be in the donor exciton state, the multipartite state of the donor-acceptor-reservoir can be expressed as

$$|\psi_t\rangle = |1\rangle_d \otimes |0\rangle_a \otimes |\mathbf{0}\rangle_r, \quad (23)$$

The presence of an exciton at the donor (acceptor) site is denoted by  $|1\rangle_d$  ( $|1\rangle_a$ ), whilst  $|0\rangle_d$  ( $|0\rangle_a$ ) denotes the absence of the exciton at the donor (acceptor) site. The reservoir state  $|\mathbf{0}\rangle_r = \prod_k |0\rangle_k$  denotes the vacuum state, while  $|\mathbf{1}\rangle_r$  is a collective state consisting of singly excited states of the form,  $|\mathbf{1}\rangle_{r_i} = \frac{1}{R_0} \sum_k \varphi_k |1_k\rangle_r$  where  $R_0 = \sqrt{\sum_k |\varphi_k|^2}$ , and states which are orthogonal to it [12].

On the basis of the quantum trajectory approach [58], dissipative processes result in the transfer of states from the exciton donor  $d$ - acceptor  $a$  subspace to the reservoir subspace. Eq. (23) evolves under the action of the Hamiltonian in Eq. (18) as

$$|\psi_t\rangle = \xi_t |1\rangle_d |0\rangle_a |\mathbf{0}\rangle_r + \eta_t |0\rangle_d |1\rangle_a |\mathbf{0}\rangle_r + \chi_t |0\rangle_d |0\rangle_a |\mathbf{1}\rangle_r, \quad (24)$$

where  $|\xi_t|^2$  ( $|\eta_t|^2$ ) is the probability that the exciton is present at the donor (acceptor) site, and  $|\chi_t|^2 = 1 - |\xi_t|^2 - |\eta_t|^2$  is the probability that the collective reservoir state is excited. For the initial condition,  $\xi_0=1$ ,  $\eta_0=0$ , and we obtain the analytical expressions,  $|\xi_t|^2 = e^{-\lambda_c t/2} [\cos \Omega t + \frac{\lambda_c}{4\Omega} \sin \Omega t]^2$ , and  $|\eta_t|^2 = e^{-\lambda_c t/2} \frac{V^2}{\Omega^2} \sin^2 \Omega t$ , where the Rabi frequency  $2\Omega = (4V^2 - (\frac{\lambda_c}{2})^2)^{1/2}$ .

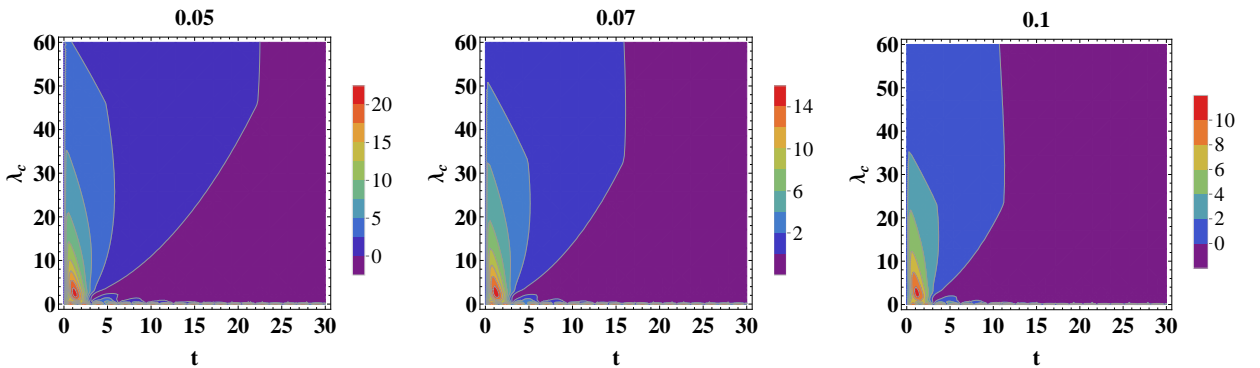


FIG. 4: Non-Markovianity in the entangled photosynthetic reaction center (RC) for a state of the form given in Eq. (25). Trace-distance difference function,  $D(t, \tau)$  (see Eq.(28)) is evaluated as a function of  $t$  and decay rate,  $\lambda_c$  for the density matrix corresponding to the exciton-donor(1)-sink(1)-sink(2) subsystem (Eq.(27)).  $a=b=\frac{1}{\sqrt{2}}$  and values of  $\tau$  are indicated at the top of each figure. Large damping ( $\lambda_c$ ) associated with higher rate of detection by the dissipative sink, appear to enhance non-Markovian dynamics (positive values of  $D(t, \tau)$ ). The unit system is based on  $\hbar = V = 1$ , with time  $t$  obtained as inverse of  $\Omega_0$  (at  $\lambda_c = 0$ )

Eq.(24) can be extended to examine the joint evolution of a pair of qubit systems (denoted) in uncorrelated reservoirs via a initial state of the form

$$|\Phi\rangle_l = a|\psi_t\rangle_1|\psi_0\rangle_2 + b|\psi_t\rangle_2|\psi_0\rangle_1 \quad (25)$$

$$|\psi_0\rangle_1 = |1\rangle_{d1}|0\rangle_{a1}|\mathbf{0}\rangle_{r1}, \quad |\psi_0\rangle_2 = |1\rangle_{d2}|0\rangle_{a2}|\mathbf{0}\rangle_{r2} \quad (26)$$

where  $i=1,2$  denote the two distinct qubits and  $a, b$  are real coefficients (as in Eq.(16)). Prominent non-Markovian features are seen (Figure 4) in the tripartite qubit associated with the donor exciton(1)-sink(1)-sink(2) partition:

$$\rho_{d_1, r_1, r_2}(t) = \begin{pmatrix} (|\eta_t|^2 + |\xi_t|^2)b^2 + a^2|\eta_t|^2 & 0 & 0 & 0 & 0 & 0 & 0 & 0 & 0 \\ 0 & b^2|\chi_t|^2 & ab|\chi_t|^2 & 0 & ab\sqrt{|\xi_t|^2|\chi_t|^2} & 0 & 0 & 0 & 0 \\ 0 & ab|\chi_t|^2 & a^2|\chi_t|^2 & 0 & a^2\sqrt{|\xi_t|^2|\chi_t|^2} & 0 & 0 & 0 & 0 \\ 0 & 0 & 0 & 0 & 0 & 0 & 0 & 0 & 0 \\ 0 & ab\sqrt{|\xi_t|^2|\chi_t|^2} & a^2\sqrt{|\xi_t|^2|\chi_t|^2} & 0 & a^2|\xi_t|^2 & 0 & 0 & 0 & 0 \\ 0 & 0 & 0 & 0 & 0 & 0 & 0 & 0 & 0 \\ 0 & 0 & 0 & 0 & 0 & 0 & 0 & 0 & 0 \\ 0 & 0 & 0 & 0 & 0 & 0 & 0 & 0 & 0 \\ 0 & 0 & 0 & 0 & 0 & 0 & 0 & 0 & 0 \end{pmatrix} \quad (27)$$

We employed the trace-distance difference

$$D(t, \tau) = \frac{D[\rho(t), \rho(t + \tau)] - D[\rho(0), \rho(\tau)]}{D[\rho(0), \rho(\tau)]} \quad (28)$$

to identify violations of the monotonically contractive characteristic features in the tripartite state of Eq.(8). The results in Figure 4 show that a large damping or decay rate ( $\lambda_c$ ) associated with the trapping process at the dissipative sink leads to an enhancement of non-Markovian dynamics in the donor exciton(1)-sink(1)-sink(2) partition,  $\rho_{d_1, r_1, r_2}(t)$  (Eq.(27)). The non-Markovian effects is pronounced at small values of  $\tau$ . The two dissipative sinks which act as indirect detectors [71], appear to induce a anti-Zeno-like effect facilitating information feedback into the specific partition considered here. This result is consistent with those in a recent work [72] where it was shown that repeated measurements in disordered systems can induce a quantum anti-Zeno effect which enhance quantum transport under certain conditions. It is important to note that the Zeno criteria used here is reliant on the detecting role of the dissipative sinks, which differs from that used in Section V in which a quantitative relation (Eq.(14)) was employed.

The observation of increased inter-qubit non-Markovian dynamics due to the dissipative sinks in the prototypical donor-acceptor-reservoir model may be applied to the larger networked systems of photosynthetic biomolecules. A quantitative assessment of the contribution from the anti-Zeno-like action of the photosynthetic sink to the efficiency of energy transfer is expected to be numerically intense involving matrix sizes larger than the tripartite state in Eq.(27) Such calculations would need to take into account extrinsic factors such as network size and topological connectivity present in the molecular structures of multichromophoric macromolecule(MCMM) systems.

As discussed in Section II, the density matrix in any physically realistic subspace, in any initially correlated system-bath state, appear not to necessitate a statistical interpretation. In general, it is desired to employ exact and non-perturbative methods to examine general non-Markovian dynamics of quantum systems. However the quantum master equation approach ((Eqs.(18),(19))) and subsequent evaluation of the density matrix of high dimensional systems of large biomolecular system present expected insurmountable challenges. In this regard, the results of the set of states for which non-positivity appears, should be compared with alternative approaches such as the non-perturbative hierarchical equations of motion (HEOM) technique [51, 52], with availability of appropriate computational resources in future works. It is hoped that the donor-acceptor-sink model used here, will serve as a starting point to comprehend the mechanisms under which non-Markovian and dissipative dynamics appear to coexist, with implications for salient properties of chemical and biological systems.

## VIII. DISCUSSION AND CONCLUSIONS

The observations of long-lasting coherence at ambient temperatures [42] in large biomolecular system have yet to be satisfactorily explained due to the sheer complexity of modeling large complex molecules against a background of noisy processes. Till now, the exact link between the robust coherence times and the time taken for excitation energy to be transferred from the antenna to the reaction center in the FMO trimer complex remains unknown. This work is a step forward in a qualitative examination of possible coordination between the observed coherence and the environment-assisted transfer mechanisms based on the Zeno-effect.

Further insight into understanding of the mechanisms in natural systems will provide innovative ways for robust control in open quantum dissipative systems. Photosynthetic complexes have been modeled as quantum channels [73] in Ref.[74], where noise-assisted energy transport have been examined in terms of transmission of classical and quantum information, via characterization by population damping and decoherence parameters. The classical and quantum channel capacities of photosynthetic complexes were seen to be enhanced by the presence of noise unlike the noiseless system with zero capacity limit.

The role of a noisy environment which acts as a detection medium with Zeno-like effects, could be further expanded for applications related to quantum control and selection of quantum channels with capacities of a quantifiable amount. The result in Figure 4, even if it is obtained for one specific partition, highlights the possibility of quantum control of energy transfer mechanisms through concatenated sequences and pulse interval optimization associated with dynamical coupling theory [75, 76], using artificial light harvesting systems. It is known that open-loop quantum optimal control techniques [77] may be utilized to verify quantum coherent transport mechanisms in light-harvesting complexes. To this end, Zeno-like effects may be incorporated in optimally shaped laser pulses [77] to initialize a photosystem, either in localized or extended mode, to discriminate different routes of transport, and to direct energy along critical pathways in light harvesting complexes. This possibility needs detailed study to seek effective quantum control for viable applications in energy systems, and especially in the regime of optimal energy transfer.

In summary, using an entangled system consisting of two spin-boson and and reservoir systems , we have identified enhanced non-Markovian signatures which can be associated with the Zeno or anti-Zeno effect depending on the subsystem under consideration. The results indicate that changes in decay rate due to the Zeno or anti-Zeno effect may be linked to non-Markovian type feedback from the system or reservoir. The time domains involved during effective Zeno or anti-Zeno dynamics is of the same order of magnitude as the non-Markovian time scale associated with the reservoir correlation dynamics. This study highlights that the context of non-Markovianity can reveal a different phenomenological perspective of the quantum Zeno/anti-Zeno effects. Consideration of the Zeno effect in a model photosynthetic system highlights enhanced inter-qubit non-Markovianity in the tripartite subsystem involving two dissipative sinks. Further investigation is needed to seek a rigorous link between the efficient rate of energy transfer in light-harvesting systems and the mechanism by which the monitoring action of the dissipative sinks results in notable non-Markovian signatures in specific partitions of multipartite states. The latter states hold much relevance in large photosynthetic membranes which constitute many FMO complexes [69], with capacity to hold a large number of entangled excitonic qubits, when conditions for occurrence of initially correlated chromophores become favourable.

## IX. ACKNOWLEDGMENTS

A. T. gratefully acknowledges the support of the Julian Schwinger Foundation Grant, JSF-12-06-0000. The author would like to thank F. Caruso and M. B. Plenio for useful comments on the initial draft of this manuscript, and the anonymous referees for helpful suggestions.

## X. REFERENCES

- 
- [1] E.C.G. Sudarshan, P.M. Mathews, J. Rau, Phys. Rev. **121**, 920 (1961).
  - [2] M. Choi, *Positive Linear Maps on  $C^*$ -Algebras*, Can. J. Math Vol.24 No.3, 520-529 (1972)
  - [3] K. Kraus, "States, Effects, and Operations: Fundamental Notions of Quantum Theory", Springer (1983)
  - [4] Nielsen, M.A., Chuang, I.L.: Quantum Computation and Quantum Information. Cambridge University Press, Cambridge (2000)
  - [5] M.M. Wolf, J. Eisert, T.S. Cubitt, J.I. Cirac, Phys. Rev. Lett. **101**, 150402 (2008).
  - [6] H.-P. Breuer, E.-M. Laine, J. Piilo, Phys. Rev. Lett. **103**, 210401 (2009)
  - [7] A. Rivas, S. F. Huelga and M. B. Plenio, Phys. Rev. Lett. **105**, 050403 (2010).
  - [8] R. Alicki, K. Lendi, Quantum Dynamical Semigroups and Applications, Lecture Notes in Phys., vol. 286, Springer-Verlag, 1987.
  - [9] E. B. Davies, Quantum Theory of Open Systems, (Academic, New York, 1976).
  - [10] G. Lindblad, Commun. Math. Phys. **48**, 119 (1976).
  - [11] A. K. Rajagopal, A. R. U. Devi, R. W. Rendell, Phys. Rev. A **82**, 042107 (2010).
  - [12] A. Thilagam and A. R. U. Devi, J. Chem. Phys. **137**, 215103 (2012).

- [13] T.F. Jordan, A. Shaji, E.C.G. Sudarshan, Phys. Rev. A **70**, 1 (2004).
- [14] P. Pechukas, Phys. Rev. Lett. **73**, 1060 (1994).
- [15] A. Smirne, H.-P. Breuer, J. Piilo and B. Vacchini, Phys. Rev. A **82**, 062114 (2010).
- [16] J. Dajka and J. Luczka, Phys. Rev. A **82**, 012341 (2010).
- [17] M. Ban, S. Kitajima, and F. Shibata, Phys. Lett. A **375**, 2283 (2011).
- [18] R. Alicki, Phys. Rev. Lett. **75**, 3020 (1995).
- [19] Pechukas, Phys. Rev. Lett. **75**, 3021 (1995).
- [20] I. Bengtsson and K. Życzkowski, *Geometry of quantum states: An Introduction to Quantum Entanglement* (Cambridge University Press, Cambridge, 2006).
- [21] W.M. Itano, D. J. Heinzen, J. J. Bollinger and D. J. Wineland, Phys. Rev. A **41**, 2295 (1990).
- [22] Nakazato H, Namiki M and Pascazio S, Int. J. Mod. Phys. B **10** 247 1996
- [23] A. G. Kofman, G. Kurizki, Nature **405**, 546 (2000); Phys. Rev. A **54**, 3750(R)(1996).
- [24] B. Misra and E. C. G. Sudarshan, J. Math. Phys. **18**, 758 (1977).
- [25] P. Facchi and S. Pascazio, J. Phys. A: Math. Theor. **41** 493001 (2008); P. Facchi and S. Pascazio, Phys. Rev. Lett. **89**, 080401 (2002).
- [26] P. Facchi, G. Marmo and S. Pascazio, Journal of Physics: Conference Series **196**, 012017 (2009).
- [27] P. Facchi and S. Pascazio, *Progress in Optics* vol 42, p 147, Ed E Wolf (Amsterdam: Elsevier) 2001
- [28] J. Schwinger, Proc. Natl Acad. Sci. USA **45** 1552, (1959); J. Schwinger, *Quantum Kinetics and Dynamics*, (New York: Benjamin), (1970).
- [29] P. Facchi, G. Marmo, S. Pascazio, A. Scardicchio and E. C. G. Sudarshan, J. Opt. B: Quantum Semiclass. Opt. **6**, S492 (2004).
- [30] S. Maniscalco, J. Piilo, K-A Suominen, Phys. Rev. Lett. **97**, 130402 (2006).
- [31] A. Thilagam, J. Phys. A: Math. Theor. **43** (2010).
- [32] P. W. Chen, D. B. Tsai and P. Bennett, Phys. Rev. B **81**, 115307 (2010)
- [33] K. Fujii and K. Yamamoto, Phys. Rev. A **82**, 042109 (2010).
- [34] M. C. Fischer, B. Gutierrez-Medina, M. G. Raizen, Phys. Rev. Lett. **87**, 040402 (2001).
- [35] A. C. Doherty and K. Jacobs, Phys. Rev. A, **60**, 2700 (1999).
- [36] A. Beige, D. Braun, B. Tregenna, and P. L. Knight, Phys. Rev. Lett. **85**, 1762 (2000)
- [37] B. H. Liu, L. Li, Y. F. Huang, C.-F. Li, G. C. Guo, E. M. Laine, H.-P. Breuer, and J. Piilo, Nature Phys. **7**, 931 (2011).
- [38] J.D. Franson, B.C. Jacobs, T.B. Pittman, Phys. Rev. A **70**, 062302 (2004).
- [39] S. Maniscalco, F. Francica, R.L. Zaffino, N. Lo Gullo, F. Plastina, Phys. Rev. Lett. **100**, 090503 (2008).
- [40] J.G. Oliveira Jr., R. Rossi Jr., M.C. Nemes, Phys. Rev. A **78**, 044301 (2008).
- [41] H. Lee, Y.-C. Cheng, G.R. Fleming, Science, **316**, 1462 (2007).
- [42] G. S. Engel, T. R. Calhoun, E. L. Read, T.-K. Ahn, T. Mancal, Y.-C. Cheng, R. E. Blankenship, and G. R. Fleming, Nature, **446**, 782 (2007).
- [43] C. Olbrich, T. L. C. Jansen, J. Liebers, M. Aghtar, J. Strümpfer, K. Schulten, J. Knoester and U. J. Kleinekathöfer, Phys. Chem. B **115**, 8609 (2011).
- [44] F. Caruso, A. W. Chin, A. Datta, S. F. Huelga, and M. B. Plenio, Phys. Rev. A **81**, 062346 (2010); F. Caruso, A. W. Chin, A. Datta, S. F. Huelga, and M. B. Plenio, J. Chem. Phys. **131**, 105106 (2009).
- [45] A. Thilagam, J. Chem. Phys. **136**, 065104 (2012).
- [46] V. Gorini, A. Kossakowski, and E. Sudarshan, Completely positive dynamical semigroups of n-level systems, Journal of Mathematical Physics, vol. 17, no. 5, pp. 821825, 1976.
- [47] G. S. Agarwal, Phys. Rev. A **2**, 2038 (1970); Phys. Rev. A **4**, 739 (1971); Phys. Rev. **178**, 2025 (1969).
- [48] D. Kohen, Marston, and D. J. Tannor, J. Chem. Phys. **107**, 5236 (1997).
- [49] P. Talkner, Ann. Phys. **169**, 390 (1986).
- [50] W. J. Munro and C. W. Gardiner, Phys. Rev. A **53**, 2633 (1996).
- [51] Y. Tanimura and R. Kubo, J. Phys. Soc. Jpn., **58**, 101 (1989).
- [52] C. Kreisbeck, T. Kramer, M. Rodríguez, and B. Hein, J. Chem. Theory Comput., **7**, 2166 (2011).
- [53] A. Shaji and E.C.G. Sudarshan, Phys. Lett. A **341**, 48 (2005).
- [54] K. Modi, C. A. Rodríguez-Rosario, Alán Aspuru-Guzik, Phys. Rev. A **86**, 064102 (2012)
- [55] E.C.G. Sudarshan, *Quantum Measurement and Dynamical Maps*, "From SU(3) to Gravity", Cambridge University Press, 433-440 (1985)
- [56] A. J. Leggett, S. Chakravarty, A. T. Dorsey, M. P. A. Fisher, A. Garg, and W. Zwerger, Rev. Mod. Phys. **59**, 1 (1995).
- [57] H. Feshbach, Ann. Phys. **5**, 357 (1958).
- [58] H.J. Carmichael, *Statistical Methods in Quantum Optics 2*, (Springer, Berlin, 2008); H. J. Carmichael, Phys. Rev. Lett. **70**, 2273 (1993).
- [59] U. Weiss, *Quantum Dissipative Systems* (World Scientific, Singapore, 1999).
- [60] A. Thilagam, J. Phys. A **45**, 444031 (2012).
- [61] P. Facchi, H. Nakazato and S. Pascazio 2001 Phys. Rev. Lett. **86** 2699 (2001).
- [62] X. Cao, J. Q. You, H. Zheng, A. G. Kofman and F. Nori, Phys. Rev. A **82**, 022119 (2010).
- [63] P. Hänggi, P. Talkner, M. Berkovec, Rev. Mod. Phys. **62** (1990) 251.
- [64] D. Xu and K. Schulten, Chem. Phys. **182**, 91 (1994).
- [65] A. Pomyalov, C. Meier and D.J. Tannor, Chemical Physics **370**, 98 (2010).

- [66] P. Reberntrost, M. Mohseni, and A. Aspuru-Guzik, *J. Phys. Chem. B* **113**, 9942 (2009).
- [67] J. Wu, F. Liu, Y. Shen, J. Cao and R. J. Silbey, *New J. Phys.***12**,105012 (2010)
- [68] X. Chen and R. J. Silbey, *J.Chem.Phys* **132**, 204503 (2010)
- [69] A. Thilagam, *J. Chem. Phys.* **136**, 175104 (2012).
- [70] A. Thilagam and J. Singh, *Phys. Rev. B* **48**, 4636 (1993).
- [71] A.R. Bosco de Magalhaes, R. Rossi Jr., M.C. Nemes *Physics Letters A* **375**, 17241728 (2011).
- [72] K. Fujii and K. Yamamoto, *Phys. Rev. A* **82** 042109 (2010).
- [73] H. Barnum, M. A. Nielsen, and B. Schumacher, *Phys. Rev. A* **57**, 4153 (1998) .
- [74] F. Caruso, S. F. Huelga and M. B. Plenio, *Phys. Rev. Lett.* **105**, 190501 (2010).
- [75] L. Viola and S. Lloyd, *Phys. Rev. A* **58**, 2733 (1998).
- [76] K. Shiokawa and D. A. Lidar, *Phys. Rev. A* **69**, 030302 (2004).
- [77] F. Caruso, S. Montangero, T. Calarco, S. F. Huelga, M. B. Plenio, *Phys. Rev. A* **85**, 042331 (2012).